Materials Science Forum Vol. 589 (2008) pp 93-98
online at http://www.scientific.net

Online available since 2008/Jun/17

Bulk ultrafine-grained Nickel consolidated from nanopowders

J. Gubicza[1,a], H.-Q. Bui[2,b], F. Fellah[2,c], N. Szász[1,d], G. Dirras[2,e]

[1]Department of Materials Physics, Eötvös University, Budapest, P.O.B. 32, H-1518, Hungary

[2]LPMTM - CNRS, Université Paris 13, 99, avenue J. B. Clément 93430, Villetaneuse, France

[a]gubicza@ludens.elte.hu, [b]bui@lpmtm.univ-paris13.fr, [c]fellah@lpmtm.univ-paris13.fr, [d]szasz.noemi1@chello.hu, [e]dirras@lpmtm.univ-paris13.fr

Keywords: nanopowders, Hot Isostatic Pressing (HIP), Spark Plasma Sintering (SPS), microstructure, mechanical properties.

Abstract. Ultrafine-grained samples were consolidated from Ni nanopowders with the nominal particle size of 50 and 100 nm by Hot Isostatic Pressing (HIP) and Spark Plasma Sintering (SPS). The higher nickel-oxide content and the smaller grain size of SPS-processed samples result in a higher yield strength at room temperature compared with HIP-processed specimen. It is found that during compression the dislocation density increases while the twins decay in both samples, indicating that the deformation is mediated mainly by dislocations. As a consequence of the higher oxide content, the flow stress of the SPS-processed samples saturates at small strain values while the HIP-processed specimen shows strain hardening even at the strain value of 0.35. After saturation of the flow stress for SPS-processed samples the deformation is most probably mediated rather by grain rotation or grain boundary-related mechanisms such as sliding and/or decohesion instead of dislocation motion.

Introduction

Bulk nanostructured or ultrafine-grained materials can be synthesized in two essentially different ways. The first one is a „top-down" approach where the bulk coarse-grained materials are refined into nanostructured materials by severe plastic deformation (SPD) [1-4].The second way for producing ultrafine-grained materials is a „bottom-up" approach when samples are assembled from individual atoms or nanoparticles [5-7]. Most „bottom-up" methods first produce nanopowders which need to be consolidated in a second step. The nanostructures obtained by powder sintering are texture-free and they have higher thermal stability compared with the SPD-processed materials. At the same time the sintered nanomaterials often have undesired contamination and remaining porosity [8]. The microstructure of the compacted ultrafine-grained materials is strongly affected by the method of consolidation. In this work the microstructure and the mechanical behavior of Ni samples produced from nanopowders under different processing conditions are studied. First, the effect of the consolidation techniques on the grain size and the defect structure are investigated by applying different compaction methods such as Hot Isostatic Pressing (HIP) and Spark Plasma Sintering (SPS). Moreover, the influence of the initial powder particle size is also studied in the case of SPS procedure. The characteristic features of the mechanical behavior of different bulk samples are related to the phase composition and microstructure.

Experimentals

Ni nanopowders with the nominal particle size of 50 and 100 nm were supplied by the Argonide Corporation (USA). The powders were produced by electro-explosion of Ni wires [9,10]. TEM images (not shown here) revealed that the powder particles have spherical shape. In the following the powders are referred as „50 nm powder" or „100 nm powder". The 100 nm powder was consolidated using HIP and SPS methods. Additionally, the 50 nm powder was compacted by SPS

procedure to study the effect of particle size on the microstructure of SPS-processed materials. Before HIP processing, the 100 nm powder was heat-treated in a capsule under hydrogen flow at 400°C and the capsule was sealed under inert gas (Ar) for preventing oxidation. During HIP method, the capsule was subjected to a pressure of 140 MPa at 700 °C for 150 min. Before SPS processing, the capsule containing the 50 or 100 nm powder was broken in air and rapidly transferred to a mould. During SPS procedure, the powder was held under a pressure of 150 MPa at 500 °C for 1 min while pulses of high current density (of the order of 1000 A/cm^2) were applied to the sample for promoting consolidation. The most important advantage of the latter method is that the compaction occurs more quickly and at much lower temperatures than in the case of classical techniques (e.g. HIP), thus preventing grain growth.

The phase composition was studied by X-ray diffraction using a Philips Xpert powder diffractometer with CuKα radiation. The microstructure was studied by transmission electron microscopy (TEM) and X-ray line profile analysis. The X-ray line profiles were measured by a high-resolution rotating anode diffractometer (Nonius, FR591) using CuKα_1 radiation. The scattered X-rays were detected by imaging plates with the angular resolution of 0.005° in 2Θ, where Θ is the angle of diffraction. The line profiles were evaluated using the extended Convolutional Multiple Whole Profile (eCMWP) fitting procedure described in detail in other reports [11,12]. This method gives the dislocation density and the probability of twins with good statistics. The latter quantity gives the fraction of the faulted 111 planes along their normal vector. The microstructure was also investigated using a JEOL-2011 transmission electron microscope operating at 200 kV. The mechanical behavior was investigated by compression (using an Instron universial testing machine, model 1195) at room temperature at a strain rate of 10^{-4} s^{-1} up to rupture.

Results and discussion

Both in the powders and the bulk samples NiO was detected beside the main Ni phase. Energy Filtered TEM images (not shown here) revealed a significant amount of oxygen located both in the surface layer and also inside the particles in the initial Ni powders when exposed to air. For comparison of the NiO phase content in the different samples, the intensity ratio of the NiO and Ni peaks at 2Θ=37.4° and 44.6°, respectively, was determined and listed in Table 1. It should be noted that this ratio does not give the NiO phase content in the samples, it is only proportional with the volume fraction of NiO phase. The intensity ratio for the initial powder with the nominal particle size of 50 nm (1.2 %) is about two times higher than that of the initial powder with the nominal particle size of 100 nm (0.5 %). The higher volume fraction of NiO in the powder having smaller particle size can be explained by that most of the oxide covers the particle surfaces. During HIP processing of 100 nm powder, the NiO content does not change because of the careful isolation of the samples from the air. On the other hand, the SPS procedure results in a significant increase of the oxide content for both 50 and 100 nm powders (see Table 1) which can be attributed to the powder processing in air before consolidation.

sample	I_{NiO}/I_{Ni} [%]	D_{TEM} [nm]	ρ [10^{14} m^{-2}]	β [%]	σ_Y [MPa]
HIP, 100 nm	0.5(1)	403	5.6(5)	0.32(2)	542(14)
SPS, 100 nm	0.9(1)	294	5.1(5)	0.29(2)	682(15)
SPS, 50 nm	1.5(1)	250	3.7(4)	0.25(2)	1022(20)

Table 1: The intensity ratio (I_{NiO}/I_{Ni}) of NiO and Ni peaks at 2Θ=37.4° and 44.6°, respectively, the mean grain size (D_{TEM}), the dislocation density (ρ), the twin probability (β) and the yield strength (σ_Y) for the samples processed by HIP and SPS.

Figure 1 shows the TEM images obtained on the bulk samples consolidated from 100 nm powder by HIP and SPS as well as processed by SPS from 50 nm powder. The mean grain size (determined from TEM) as well as the densities of dislocations and twins are listed in Table 1. It is revealed that the high temperature consolidation results in grain coarsening. The grain-growth is moderated in the case of SPS procedure due to the reduced temperature and time of processing. TEM and X-ray line profile analysis show that the twin density decreases from 2-3% to 0.2-0.3% during compaction either by HIP or SPS method. At the same time, while dislocations were not detected in the intital powders, during compaction a significant amount of dislocations was formed. This indicates that high temperature plastic deformation during consolidation is basically mediated by dislocations.

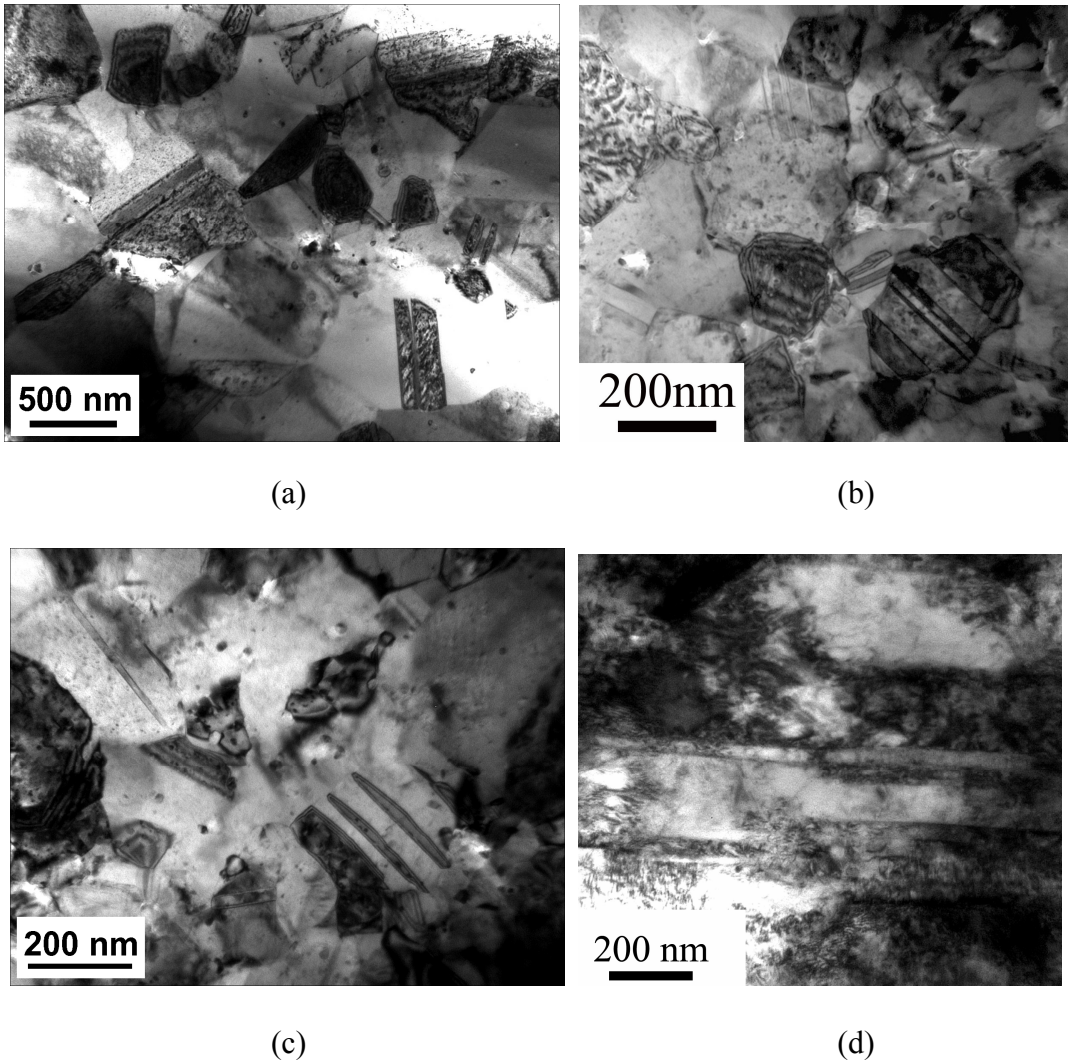

Fig. 1. TEM images for the bulk samples consolidated by (a) HIP from 100 nm powder, (b) SPS from 100 nm powder, (c) SPS from 50 nm powder and (d) specimen processed by HIP from 100 nm powder after the failure in compression test.

The three bulk samples were tested by compression until the failure of the specimens. The true stress vs. true strain curves are presented in Fig.2. The yield strength values determined at 0.2% plastic strain are listed in Table 1. The sample processed from 100 nm powder by SPS has higher yield strength than that obtained from the same powder by HIP method as a result of the higher oxide dispersoid content and the smaller grain size of the former specimen. The sample processed from 50 nm powder by SPS procedure has the highest yield strength as this material has the highest oxide content and the smallest grain size among the three samples. Comparing the mechanical behavior of the samples produced from 100 nm powder, it is revealed that the HIP-processed

sample shows a hardening in the whole range of strain while in the case of SPS-processed specimen the flow stress saturates at small strain value and after that it softens slightly till the rupture. The microstructural investigations show that the dislocation density increases from 5.6 to $16x10^{14}$ m^{-2} in the case of HIP-processed sample and from 5.1 to $21x10^{14}$ m^{-2} for SPS-processed specimen. At the same time the twin probability decreases during the room temperature deformation from 0.32 to 0.02% in the case of HIP-processed sample and from 0.29 to 0.18% for SPS-processed specimen. In the case of the sample produced from 50 nm powder by SPS, the dislocation density increases from 3.7 to $8.5x10^{14}$ m^{-2} and the twin probability decreases from 0.25 to 0.20% in the compression test. The smaller changes of defect densities in this case can be explained by the very small value of strain to failure. The reduction of twin density during compression is a consequence of a reaction between moving dislocations and twins. The disappearance of twin boundaries has also been reported during nanoindentation experiments of electrodeposited Cu at room temperature [13].

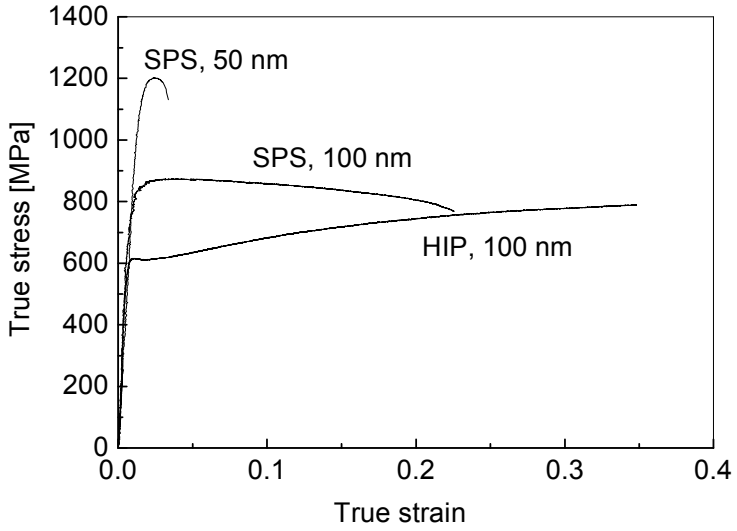

Fig. 2. True stress-true strain curves obtained by compression for the samples processed by HIP from 100 nm powder and by SPS from 100 and 50 nm powders.

During deformation of the consolidated samples, dislocations are emitted from grain boundaries and they interact with the oxide particles leaving dislocations loops around the dispersoids as revealed by TEM experiments. For example, Fig.3a shows the microstructure of the sample processed from the 50 nm powder by SPS method. In the grain on the right part of the image, the elongated objects with dark contrast represent dislocation loops. Tilting the sample by 2 degrees (see Fig.3b), only small dark spots can be seen at the places of the former loops which indicates that the loops are formed around oxide dispersoids. With increasing strain, the number of loops increases and the stress field of these loops hinders the emission of new dislocations from the grain boundaries. Therefore, the dislocation density saturated at a relatively low strain value for the SPS-processed samples where the NiO content is relatively high. It is noted that the low strain value at saturation does not exclude a high value of the saturated dislocation density as can be seen in the case of the sample produced from 100 nm powder by SPS ($21x10^{14}$ m^{-2}). As the dislocation emission from the grain boundaries is hindered in the SPS-processed specimen, the further plastic deformation is most probably mediated rather by grain rotation or grain boundary-related mechanisms such as sliding and/or decohesion. This is also confirmed by the TEM images where the deformed HIP-sample contains dislocations arranged into tangles (see Fig.4a) while the deformed SPS-samples (processed either from 50 or 100 nm powders) contain mainly numerous isolated dislocation loops (see Figs. 3 and 4b). The stress field created by dislocation loops around oxide particles may also result in the formation of voids between the Ni matrix and the dispersoids

in addition to voids at grain boundary junctions, which may contribute to the slight strain-softening in the case of SPS-sample. The relatively small grain size of the SPS-sample may also cause the lack of strain hardening as it has been shown by other authors that under a certain grain size limit (cca. 40 nm) the main deformation mechanism is rather grain boundary rotation/sliding and twinning instead of dislocation activity even in the materials where the grains do not contain oxide dispersoids.

For the samples produced from 100 nm powder, the reduction of twins is lower for the SPS-processed sample than in the case of HIP. This can be explained by the smaller value of strain to failure for the SPS-processed sample and the contribution of grain rotation or grain boundary-related mechanisms to deformation instead of dislocation activity.

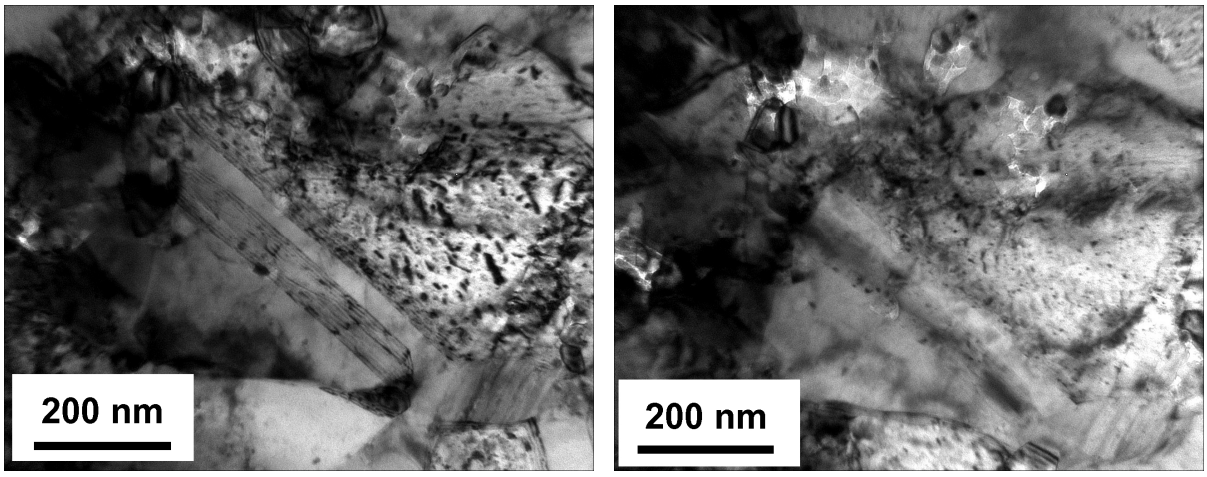

(a) (b)

Fig. 3. TEM image of the sample processed from 50 nm powder by SPS after deformation (a). The image (b) is obtained from the same area by tilting the sample by 2 degrees.

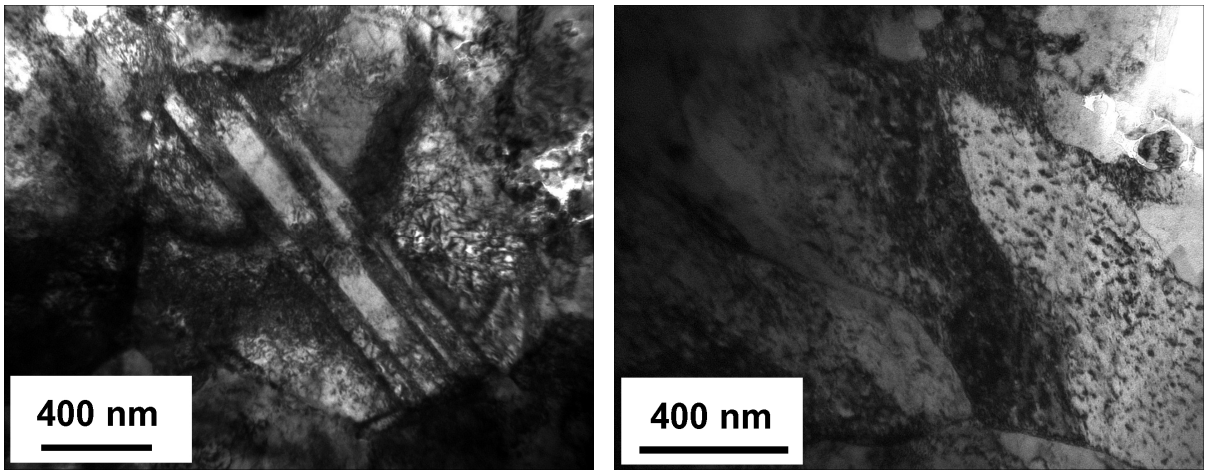

Fig. 4. TEM images for the samples processed from 100 nm powder by HIP and SPS after deformation.

Summary

Ultrafine-grained Ni samples were sintered from nanopowders. The effect of the mean particle size of the starting powder and the consolidation conditions on the microstructure and the mechanical behavior was studied. It was found that using the same intial powder, the Spark Plasma Sintering method results in a higher oxide phase content and a smaller grain size compared with Hot Isostatic Pressing. The higher concentration of oxide dispersoids yields to a higher strength and an early saturation of the flow stress during compression of SPS-processed sample. The HIP-processed sample shows a work-hardening behavior up to the rupture of the specimen. The twin density decreases during deformation of the consolidated samples as a consequence of the interaction between twins and gliding dislocations. In the case of SPS-processed samples, the dislocation loops formed around oxide dispersoids in the beginning of deformation hinder the emission of dislocations from grain boundaries resulting in the early saturation of the flow stress. The further deformation of the SPS-processed samples is probably mediated mainly by grain rotation and/or grain boundary-related mechanisms. The application of smaller intial particle size increases the oxide content yielding to the higher strength of bulk sample.

Acknowledgements

The authors are grateful for the support of the hungarian TeT Fundation (KPI) under the contract No. F-47/2006 (Balaton project). This work was supported by the Hungarian Scientific Research Fund, OTKA, Grant Nos. K67692 and K71594. JG is grateful for the support of a Bolyai Janos Research Scholarship of the Hungarian Academy of Sciences. G. Dirras is grateful for the support of EGIDE, in the framework of the Hubert Curien Project (PHC Balaton). Part of this work was also supported by the RNMP Project „AGUF" in collaboration with Arcelor.

References

[1] V.M. Segal: Mater. Sci. Eng. A Vol. 197 (1995), p. 157

[2] R.Z. Valiev, R.K. Islamgaliev, I.V. Alexandrov: Prog. Mater. Sci. Vol. 45 (2000), p. 103

[3] R.Z. Valiev, Y. Estrin, Z. Horita, T.G. Langdon, M.J. Zehetbauer, Y.T. Zhu: JOM Vol. 58 (2006), p. 33

[4] A. Dubravina, M.J. Zehetbauer, E. Schafler, I.V. Alexandrov: Mater. Sci. Eng. A Vol. 387-389 (2004), p. 817

[5] P.G. Sanders, C.J. Youngdahl, J.R. Weertman: Mater. Sci. Eng. A Vol. 234–236 (1997), p. 77

[6] H.V. Atkinson, S. Davies: Metall. Mater. Trans. A Vol. 31 (2000), p. 2981

[7] S. Billard, G.F. Dirras, J.P. Fondere, B. Bacroix, in: Proceedings of the 2nd international conference on nanomaterials by severe plastic deformation: fundamentals – processing – applications, edited by M.J. Zehetbauer, R.Z. Valiev, Wiley–VCH, Weinheim (2004) pp. 564.

[8] J. Gubicza, G. Dirras, P. Szommer, B. Bacroix: Mater. Sci. Eng. A Vol. 458 (2007), p. 385

[9] F. Tepper: Met. Powder Rep. Vol. 53 (1998), p. 31

[10] Y. Kwon, Y. Jung N. Yavorovsky, A. Illyn: Scripta Mater. Vol. 44 (2001), p. 2247

[11] G. Ribárik, J. Gubicza, T. Ungár: Mater. Sci. Eng. A Vol. 387-389 (2004), p. 343

[12] L. Balogh, G. Ribárik, T. Ungár: J. Appl. Phys. Vol. 100 (2006) 023512

[13] L. Lu, R. Schwaiger, Z.W. Shan, M. Dao, K. Lu, S. Suresh: Acta materialia, Vol. 53 (2005), p. 2169